HHS Public Access

Author manuscript

ACS Biomater Sci Eng. Author manuscript; available in PMC 2018 February 28.

Published in final edited form as:

ACS Biomater Sci Eng. 2016 November 14; 2(11): 1914–1925. doi:10.1021/acsbiomaterials.6b00274.

Vascular Network Formation by Human Microvascular Endothelial Cells in Modular Fibrin Microtissues

Ramkumar Tiruvannamalai Annamalai, **Ana Y. Rioja**, **Andrew J. Putnam**, and **Jan P. Stegemann***

Department of Biomedical Engineering, University of Michigan, Ann Arbor

Abstract

Microvascular endothelial cells (MVEC) are a preferred cell source for autologous revascularization strategies, since they can be harvested and propagated from small tissue biopsies. Biomaterials-based strategies for therapeutic delivery of cells are aimed at tailoring the cellular microenvironment to enhance the delivery, engraftment, and tissue-specific function of transplanted cells. In the present study, we investigated a modular tissue engineering approach to therapeutic revascularization using fibrin-based microtissues containing embedded human MVEC and human fibroblasts (FB). Microtissues were formed using a water-in-oil emulsion process that produced populations of spheroidal tissue modules with a diameter of 100–200 μm. The formation of MVEC sprouts within a fibrin matrix over 7 days in culture was dependent on the presence of FB, with the most robust sprouting occurring at a 1:3 MVEC:FB ratio. Cell viability in microtissues was high (>90%) and significant FB cell proliferation was observed over time in culture. Robust sprouting from microtissues was evident, with larger vessels developing over time and FB acting as pericyte-like cells by enveloping endothelial tubes. These neovessels were shown to form an interconnected vascular plexus over 14 days of culture when microtissues were embedded in a surrounding fibrin hydrogel. Vessel networks exhibited branching and inosculation of sprouts from adjacent microtissues, resulting in MVEC-lined capillaries with hollow lumens. Microtissues maintained in suspension culture aggregated to form larger tissue masses (1–2 mm in diameter) over 7 days. Vessels formed within microtissue aggregates at a 1:1 MVEC:FB ratio were small and diffuse, whereas the 1:3 MVEC:FB ratio produced large and highly interconnected vessels by day 14. This study highlights the utility of human MVEC as a cell source for revascularization strategies, and suggests that the ratio of endothelial to support cells can be used to tailor vessel characteristics. The modular microtissue format may allow minimally invasive delivery of populations of prevascularized microtissues for therapeutic applications.

Graphical abstract

*Corresponding Author: Jan P. Stegemann, Department of Biomedical Engineering, University of Michigan, 1101 Beal Ave., Ann Arbor, MI 48109, Tel: 734-764-8313, Fax: 734-647-4834 jpsteg@umich.edu.

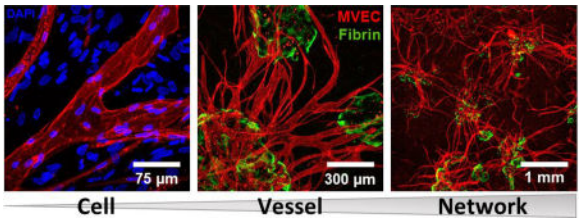

Keywords

Modular tissue engineering; vascularization; microvascular endothelial cells; fibrin; fibrinogen; microtissues; minimally invasive delivery; injectable scaffolds

Introduction

Tissues and organs in the body are permeated by a branched microvasculature that is spaced to provide efficient mass transfer[1]. These vascular networks mediate metabolism, immune response, homeostasis, regeneration and many other vital functions in tissues. When the vascular bed is damaged or non-functional, tissue function is compromised and pathological sequelae can result. In critical limb ischemia, severe obstruction of the vascular supply to the extremities can result in pain, ulcers, and eventual gangrene. A functioning vascular bed is also important when creating larger engineered tissues and organs, to support the metabolic load of the tissue-specific cells. Vascularization through incorporation of isolated vascular cells or a preformed vascular infrastructure can promote neovascularization and functional anastomoses[2–4] in both native and engineered tissues. However, there is a need to develop strategies for rapid revascularization of ischemic tissues and to enhance the vascular engraftment of engineered tissues.

Delivery of cells in defined biomaterial microenvironments has the potential to enhance survival, engraftment, and function of transplanted cells. As depicted in Figure 1, modular tissue engineering is a biomaterials-based strategy to create thick tissues through bottom-up assembly of microscale modules comprised of cells, biomaterials, and biochemical supplements[5]. In addition to facilitating minimally invasive delivery of cells and matrix, the modular approach helps to preserve cell functionality and mimics the tissue architecture, providing control over the spatial distribution of the cellular components and high mass transfer rates. Modular strategies have been developed to generate specific tissues[6–10] and complex organs[11], as well as to address the challenge of vascularization[12–15].

An appropriate cell source is a key consideration in engineered revascularization strategies. Angiogenesis (new vessels sprouting from a pre-existing vessel)[16–17], and vasculogenesis (de novo formation of vessels from endothelial progenitor cells)[18] are the two principle processes by which new blood vessels are formed. To facilitate these processes, endothelial cells (EC) rely on the degradative action of a range of secreted and membrane-bound matrix metalloproteinases (MMPs) to allow them to move through the extracellular matrix (ECM)[19–20]. Pericytes have been shown to be important in this process, and particularly in vessel stabilization and maturation[21–22]. Other cells including fibroblasts[14], mesenchymal stem cells[23], and smooth muscle cells[24] have also been used to replicate the function of

pericytes in vascularization strategies, though their exact mechanisms of action are still not well understood.

The choice of endothelial cell source is of particular importance because of their critical role in guiding and forming new blood vessels. These cells are highly immunogenic and therefore autologous sources offer the most promise in therapeutic applications. Human umbilical vein endothelial cells (HUVEC) have been used widely as a model system in vitro, due to their ready availability and demonstrated ability to form neovasculature. However, there is evidence that these macrovascular cells may differ from microvascular endothelial cells (MVEC) in terms of cytoskeletal and secreted proteins[19–21]. Furthermore, it has been suggested that there may be phenotypic differences between arterial and venous endothelial cells[25–27], and that MVEC express specific tight junction proteins required to regulate capillary permeability[26]. Importantly, MVEC can be safely be harvested from a small skin or other biopsy[28–30], though they require expansion to obtain clinically relevant numbers. They therefore present a potential autologous source of cells with a microvascular phenotype conducive to creating stable and selectively permeable vessels.

Biomaterial-mediated cell delivery has the advantage that the cellular environment can be tailored to promote desired cell functions, as well the engraftment and survival of transplanted cells. A variety of natural and synthetic polymers have been used for this purpose (reviewed by *Nair, et al.*[31]) and the clotting protein fibrin has found particular utility in supporting angiogenesis and vasculogenesis[14, 32]. Polymerized fibrin and its precursor fibrinogen play important and overlapping roles in blood clotting, cell adhesion and migration (reviewed elsewhere[33–34]), tissue morphogenesis, and wound healing[35]. Fibrinogen can be harvested from a patient's own blood, providing an abundant source while avoiding immune complications [36]. Fibrin has been widely investigated as a matrix in creating vascularized engineered tissue constructs, including for bone[7, 37–40], cartilage[41–43], adipose tissue[44–46], liver[47], pancreas[48], skin[49–50], muscle[51], and cardiovascular tissues[52–55]. In addition, the porosity, mechanical properties [56–57], and degradation rate [58–59] of fibrin can be controlled in a variety of ways. These features make fibrin an attractive extracellular matrix for the delivery of therapeutic vascularizing cells.

In the present study we fabricated and characterized discrete microtissues composed of MVEC and fibroblasts (FB) co-embedded in a fibrin matrix. A water-in-oil emulsification technique was used to create these vascular tissue modules, which could be collected and cultured as a population. The influence of culture medium volume and cell ratio (MVEC:FB) on endothelial sprouting from microtissues was investigated by quantifying cell viability, proliferation, as well as neovessel characteristics. Network formation through the inosculation of vessels between adjacent microtissues was also assessed. The purpose of this study was to investigate the utility of MVEC in creating vascular segments within microtissues, and to thereby demonstrate MVEC as a potential autologous cell source in modular tissue engineering. Our long term goal is to deliver autologous vascular microtissues in a minimally invasive manner for the therapeutic revascularization of ischemic tissues.

Material and Methods

2.1 Biopolymers and Cell culture

Fibrinogen (Fg) from bovine plasma (Sigma, St. Louis, MO) with a molecular weight of 340 kDa and ≥75 % clottable protein was used for our studies. Fg stock solution of 4.0 mg/ml (0.4 wt%) clottable proteins was made by dissolving lyophilized fibrinogen in serum free culture media at 37°C. Completely dissolved Fg solution was then sterile filtered using 0.22 μm low-protein-binding polyethersulfone (PES) membrane filters (Millex, Billerica, MA) and used for casting bulk gels and microtissues. Thrombin from bovine plasma (Sigma) with a stock concentration of 50 U/mL was used to make fibrin hydrogels.

Human neonatal foreskin microvascular endothelial cells (MVEC) and normal human lung fibroblasts (FB, passage 9–12) were obtained from a commercial vendor (Lonza Inc., Walkersville, MD). MVEC were expanded using EGM-2MV media supplemented with growth factors (BulletKit, Lonza) and FB were expanded using M199 media (Gibco Life Technologies, Carlsbad, CA) supplemented with 10% fetal bovine serum (FBS, Gibco) and penicillin (50 U/mL)/streptomycin sulfate (50 μg/100mL, Gibco). MVEC from passage 2–5 and FB from passage 9–12 were maintained at 37°C in standard cell culture incubators and the medium was replenished every two days. For MVEC-FB co-cultures, only MVEC growth media was supplied. For suspension cultures, discrete microtissues were suspended in 1.0 mL of MVEC growth media and maintained in 15 mL vented polypropylene bio-reaction tubes (Celltreat, Shirley, MA).

2.2 Bulk gel and microtissue fabrication

Cells were suspended in fibrin hydrogel solution at a total density of 2.0×10^6 cells/mL and made into discrete microtissues (~200 μm in diameter) using a water-in-oil emulsification procedure shown schematically in Figure 2 and described previously[13]. To make 1.0 mL of cellular fibrin suspension, the following components were added to a cell pellet: 255 μL of serum free culture media, 625 μL Fg stock solution (2.5 mg/mL final), 100 μL of FBS (10 vol% final), and 20 μL of 50 U/mL thrombin (1 U/mL final. The well-mixed liquid cell-matrix suspension was then injected quickly into 75 mL of stirred polydimethylsiloxane (PDMS, PMX-200, 100 cS; Xiameter Dow Corning, Midland, MI) kept in ice. Emulsification was carried out at an impeller speed of 600 rpm for 5 min on ice. The temperature of the PDMS bath was then raised to 37°C to facilitate gelation of the protein matrix. The resulting microtissues consisted of cells encapsulated in gelled fibrin droplets, which were separated from the oil phase by adding 10 ml of 10 mM PBS containing surfactant (0.1% L101, BASF, Florham Park, NJ), followed by mixing and centrifugation at 200 × g for 5 min. Microtissues were washed twice and maintained under standard culture conditions for further experiments. Bulk hydrogel constructs served as controls. To prepare control bulk hydrogel constructs, 0.5 mL of the cell-matrix suspension with the same composition as described above was poured into the wells of a 24-well plate and allowed to gel at 37°C for 30–45 min. Complete MVEC growth media was then added on top of the gel and maintained under normal culture conditions. For sprouting and proliferation assays, discrete fibrin microtissues were embedded in a larger acellular fibrin gel (0.5 ml for each well of 24-well plate) with the same composition as described above.

2.3 Cell viability and proliferation

To determine the viability of cells after encapsulation in microtissues and control bulk gels, Live/Dead® Viability/Cytotoxicity Kit (Molecular Probes, Life Technologies, Grand Island, NY) was used. DAPI (Molecular Probes).was used as a nuclear counter-stain. Samples were collected and washed in 10 mM PBS and incubated in staining solution with a final concentration of 1 μM Calcein-AM, 2 μM ethidium homodimer and 2 ng/mL DAPI at 37°C for 45 min. After two washes in 10 mM PBS, samples were resuspended in fresh PBS and imaged with an inverted fluorescence microscope (Nikon) using appropriate filter sets (Excitation/Emission 488/520 for calcein-AM, 528/617 for ethidium homodimer and 350/470 for DAPI).

Cell proliferation was determined by quantifying total DNA in samples using a commercially available double stranded-DNA assay kit (Quanti-iT™ PicoGreen, Invitrogen, Life Technologies, Grand Island, NY). To isolate the total DNA from samples, fibrin gels containing microtissues were suspended in ice-cold 10 mM Tris-HCL/0.4 M guanidine hydrochloride solution (pH-7.5) and homogenized using a probe sonifier (Branson Ultrasonics, Danbury, CT) for 20 s, with a 10 s interval to avoid heat denaturation. The digested samples were then centrifuged at $10^4 \times g$ for 10 min and the supernatant containing the DNA was aspirated and then diluted with water to reduce guanidine-HCl interference with the DNA assay. DNA content was determined using the PicoGreen® DNA assay kit (Invitrogen). Calf thymus DNA standards (Invitrogen) were used to generate standard curves.

2.4 Confocal imaging and analysis of endothelial sprouts

Confocal images of bulk gels, discrete microtissues, and gel-embedded microtissues were captured using a Nikon A1 confocal laser microscope. All the acquired optical sections were processed using Fiji (Image J) software (National Institutes of Health). For sprouting analysis in bulk gels, the number of sprouts and the average length of the sprouts per unit area were measured using a protocol similar to previous studies [56, 60–62]. Samples were collected in triplicates at specific time intervals and fixed using a buffered alcoholic formalin solution (Z-Fix, Anatech Ltd, Battle Creek, MI). After washing twice in PBS, the sprouts were stained with the endothelial cell-specific marker Ulex Europaeus Agglutinin I (UEA-I, Vector Laboratories, Burlingame, CA). DAPI (Molecular Probes) was used as nuclear counter-stain. Samples were washed twice in 10 mM PBS and then incubated in staining solution with a final concentration of 1% BSA (non-specific blocker), 10 μg/ml rhodamine-labeled UEA-I and 2 ng/mL DAPI for 45 min at 4°C. After rinsing twice in 10 mM PBS, samples were resuspended in fresh PBS and z-stacked images were captured. Elongated tubular structures, positive for UEA-1 and >100 μm in length were considered sprouts and quantified for comparison between conditions.

For sprouting analysis of the embedded cultures, discrete fibrin microtissues were embedded in a larger acellular fibrin gel. Prior to embedding, microtissues were labelled by incubating them in a FITC-conjugated fibrinogen solution (9 μg/mL in PBS, Life Technologies) at 37°C for 45 min. The labelled fibrinogen allowed distinction between the microtissues and surrounding acellular matrix. After gelation, culture media was added on top of the bulk gels

and maintained under normal culture conditions. Samples were collected in triplicates at specified time intervals and fixed using a buffered alcoholic formalin solution (Z-Fix). After fixation, the sprouts were stained using UEA-1 and DAPI as describe above. After rinsing twice in 10 mM PBS, samples were resuspended in fresh PBS and images were captured using a confocal microscope (Nikon A1) with appropriate lasers (Excitation/Emission 488/520 for FITC-AM, 528/617 for UEA-1 and 350/470 for DAPI). Confocal stacks of the microtissues (1024px – 1.275 mm^2) with sprouts were merged (Z project), and the total vessel area and the average diameter of the sprouts were measured using a protocol similar to previous studies [56, 60–62]. For vessel diameter measurements, the region of interest (ROI) was restricted to a 1 mm diameter circular area with the microtissues as its center. Binary threshold maps of the images were used to measure area of the vessel regions.

2.5 GFP-transduction

For confocal microscopy and flow analysis, FB were stably transduced with a lentiviral vector expressing GFP (sc-108084, Santa Cruz, Dallas, Texas) designed to self-inactivate after transduction and integration of copGP constructs into the genomic DNA of target cells. The cells to be transduced were seeded into six-well plates at a density of 1000 cells/cm^2 and cultured overnight. The following day, viral particles were added to the cells at a MOI of 4.0 and incubated at 37°C. A complete media change was done after 24 hours and stably transfected cells were then selected using 6.0 μg/mL puromycin treatment. Highly fluorescent cells were then sorted out using a MoFlo Astrios EQ (Beckman Coulter) instrument, and were subsequently used for further experiments.

2.6 Flow cytometry

Samples were collected at day 0, 7 and 14, washed twice in PBS and digested in 1 mL of 1.0 mg/mL collagenase (MP Biomedical, Santa Ana, CA) in Ca^{2+}/Mg^{2+} free HBSS solution at 37°C in a humidified chamber for 60 min to obtain a single cell suspension. For flow analysis, GFP-transduced FB were used. MVEC were labelled with the endothelial cell-specific marker UEA-I conjugated to rhodamine (Vector Laboratories) and dead cells were excluded using 2 ng/mL DAPI (Molecular probes). All cell labelling was done in the dark on ice in cold FACS buffer (PBS, 7% FBS, 0.1% NaN_3 sodium azide (sigma)). The samples were then washed twice in PBS, filtered through 80 μm nylon mesh and analyzed in a Coulter Cyan #5 analyzer (Beckman Coulter, Miami, FL). Data were exported as FCS files and analyzed using Summit 4.3 (Beckman Coulter, Inc. Fullerton, CA). Pure populations of GFP transduced FB and MVEC were used as positive control.

2.7 Histology and immunohistochemistry

Microtissue samples were collected at day 7 and day 14 and fixed overnight using a buffered alcoholic formalin solution (Z-Fix, Anatech). The samples were then infiltrated with paraffin using an automated tissue processor (TP1020, Leica Biosystems, Buffalo Grove, IL), embedded in paraffin blocks and cut into 5 μm sections using a rotary microtome. Deparaffinized and hydrated sections were stained with hematoxylin and eosin (H&E) and mounted using toluene. For immunohistochemistry (IHC), an antibody against endothelial surface marker CD31/PECAM-1 (polyclonal IgG, Santa Cruz) was used at 1:50 dilution. Sections were treated with Proteinase K (Digest-All™, Life Technologies) for 10 min to

retrieve antigens and blocked with SuperBlock (Life Technologies) to prevent non-specific antibody binding, and with Peroxidase Suppressor (Life Technologies) to quench endogenous peroxidase. Following primary and HRP-conjugated secondary antibody incubation, diaminobenzidine (DAB; Sigma) was used as a chromogen and hematoxylin for counterstaining. The sections were then mounted and imaged with a brightfield microscope (Nikon).

2.8 Statistics

All measurements were performed at least in triplicate. Data are plotted as means with error bars representing the standard deviation. The Pearson correlation coefficient (r) was used to evaluate linear correlation between two variables. Statistical comparisons were done using Student's t-test with a 95% confidence limit (two-tailed and unequal variance). Differences with $p<0.05$ were considered statistically significant.

Results

3.1 Characterization of sprout formation in bulk gels

The influence of cell ratio and media volume on MVEC sprouting was initially investigated in bulk hydrogel cultures. Three MVEC:FB ratios (1:0, 1:1, and 1:3) and three supernatant medium volumes (0.25, 0.50, and 1.0 mL) were examined, using hydrogels made at a total cell concentration of 2.0×10^6 cells/mL and a one week culture period. Figure 3 shows the qualitative and quantitative data on the extent of endothelial sprout formation in the nine conditions tested. Confocal images (Fig. 3A) showed that MVEC embedded without FB (1:0 condition) showed essentially no sprout formation, regardless of medium volume. Sprouting generally increased as the ratio of MVEC to FB decreased, and as the volume of supernatant medium used increased.

Quantification of the extent of sprout formation confirmed the qualitative observations. The number of sprouts >100 μm in length (Fig. 3B) was very small in pure MVEC cultures. The number of sprouts increased at the 1:1 cell ratio, with significantly higher numbers seen at the 0.5 and 1.0 ml medium volumes conditions compared to the 0.25 ml volume ($p<0.001$). The 1:3 cell ratio cultures exhibited the highest number of sprouts per unit area, with significantly more sprouts seen in the 1.0 ml medium volume as compared to the 0.25 and 0.5 ml volumes ($p<0.001$). The correlation between treatments (Table I) showed a strong linear trend between culture medium volume and the number of sprouts at the 1:3 cell ratio ($r=0.95$), while no strong correlation was seen between any other treatments. Although there was a general increase in the number of sprouts with decrease in MVEC:FB ratio, the observed correlation was not strong.

The total number of sprouts over a week in culture (Fig. 3C) exhibited a trend similar to the average sprout length. In pure MVEC cultures, the few sprouts observed were generally less than 20 μm in length. When FB were added, sprout length increased markedly. The 1:1 cell ratio exhibited robust sprouting with lengths averaging ~140 μm. However, no statistical significance across medium volumes was observed. The 1:3 cell ratio generated the longest sprouts, generally averaging between 150–250 μm. Cultures maintained in 1.0 ml of medium

produced longer sprouts (~240 μm) than those maintained in 0.25 ml (~170 μm, $p<0.01$) or 0.5 ml (~195 μm, $p<0.05$) of medium. The correlation analysis (Table II) between conditions showed a strong direct correlation ($r>0.94$) between a higher FB content and average sprout length at all medium volumes. The average sprout length was also positively correlated with supernatant medium volume at all ratios, while the linear correlation was statistically significant ($p<0.01$) only in 1:3 cell ratio cultures.

3.2 Cell viability and proliferation of cells within microtissues

Because of the clear positive influence of FB on sprout formation in bulk gels, the 1:1 and 1:3 cell ratios were used to fabricate 3D fibrin microtissues. The total cell density in microtissues was maintained at 2.0×10^6 cells/ml. Figure 4A shows representative phase contrast images of a single microtissue at each cell ratio, with the embedded cells visible in the microtissue matrix. The viability of cells immediately after encapsulation was assessed using a vital stain (Fig. 4B), and revealed very little cell death. Quantification of a population of microtissues (Fig. 4C) showed that cell viability was high and statistically the same at both cell ratios (94.6% for 1:1 and 96.1% for 1:3), and was not different from viability in corresponding bulk hydrogels (data not shown). Similarly, the total number of cells encapsulated per unit volume of the microtissues at day 0, was statistically the same at both cell ratios (Fig. 4D).

Proliferation of cells incorporated into the microtissues (Fig. 4E) was examined by measuring the total DNA content over time in culture. At day 0, the total DNA content at 1:1 and 1:3 cell ratios was statistically the same. The amount of DNA in both microtissue types increased with time, indicating proliferation of cells within the matrix. However, the rate of proliferation was different between cell ratios. By day 7 the 1:1 cell ratio microtissues contained 37% more DNA than the 1:3 microtissues ($p<0.001$), and by day 14 the 1:1 cell ratio microtissues contained 52% more DNA than the 1:3 microtissues ($p<0.001$), indicating significantly higher cell proliferation at the higher MVEC:FB ratio.

The population dynamics of MVEC and FB in the microtissues over time was investigated using flow cytometric analysis, as shown in Figure 5. UEA-I conjugated with rhodamine was used to identify MVEC, while FB were transduced with GFP for easy identification (Fig. 5A, B). Flow cytometric analysis of microtissue samples digested immediately after seeding revealed cell ratios similar to that of the seeding ratios (Fig. 5C, D), as expected. However, over time there was a clear preferential proliferation of FB, such that by day 7 the corresponding ratios had decreased to 1:2 (25.8±1.07 % MVEC, 53.9±1.81 % FB) and 1:4 (15.1±2.5 % MVEC, 63.4±4.4 % FB), as shown in Figures 5E and 5F. This shift was even more pronounced by day 14 with the respective ratios further decreasing to 1:2.5 (21.2±2.8 % MVEC, 54.6±4.33 % FB) and 1:6 (10.8±0.32 % MVEC, 69.4±0.58 % FB), as shown in Figures 5G and 5H. Labelled MVEC and FB were also used to examine the spatial organization of cells in cocultures, as shown in Figure 6. At both the 1:1 and 1:3 MVEC:FB ratios, there was a clear pattern of FB organizing around the periphery of formed and forming endothelial tubes.

3.3 MVEC sprouting from microtissues

Microtissues containing MVEC and FB were embedded in a surrounding acellular fibrin gel to examine endothelial sprouting over two weeks in culture. Figure 7A shows representative microtissues made with either 1:1 or 1:3 MVEC to FB ratios, in which the fibrin used to fabricate the microtissue was labeled green, while the surrounding fibrin was unlabeled. In both microtissue types, robust endothelial sprouting into the surrounding matrix was observed by day 7. These vessels were maintained over time in culture and at day 14 had a more mature appearance than at earlier time points. Quantification of the vessel area relative to the microbead area in images (Fig. 7B), showed that vessel size remained relatively constant over two weeks in culture in the 1:1 ratio microtissues, but that vessel size increased significantly over time in the 1:3 ratio microtissues ($p<0.001$). The vessels in the 1:1 ratio microtissues were smaller than those in the 1:3 ratio microtissues at day 7, but by day 14 there was no significant difference between the conditions.

The diameter of endothelial sprouts was measured and expressed in box plots in Figure 7C to allow examination of the population distribution of the neovessels, and average diameters are provided in Table III. At day 7 of embedded culture, sprouts from the 1:1 microtissues exhibited a relatively uniform distribution of vessel diameter with a mean of 24±12 μm. The microtissues at the 1:3 cell ratio exhibited a slightly wider distribution of vessel sizes with a mean diameter of 25±18 μm. By day 14, the size distributions were markedly more skewed toward larger vessels. The 1:1 microtissues had mean vessel diameter of 33±26 μm, which was not statistically significantly different from day 7. In contrast, by day 14 the 1:3 microtissues increased in average diameter to 48±38 μm, which was statistically greater than the 1:1 microtissues at day 14 ($p<0.05$) and the 1:3 microtissues at day 7 ($p<0.001$). Of note was the number of larger vessels with diameter greater than 100 μm in the day 14 samples, particularly at the 1:3 MVEC:FB ratio.

3.4 Inosculation of neovessels and network formation

Populations of microtissues embedded in acellular fibrin began to form primitive vessel networks through the inosculation of endothelial sprouts from adjacent microtissues.

Figure 8 shows representative fluorescence images of vessel networks formed by microtissues. Clear interaction between sprouts is seen at day 7 (Fig. 8A), and this process continued to form more extensive networks by day 14 (Fig 8B). More detailed examination of anastomosing neovessels was performed using higher magnification fluorescence imaging and histological sectioning, as shown in Figure 9. A collection of inosculating vessels from three different microtissues is shown in Fig 9A(i), and a confocal image stack of a specific branch point is shown in Fig 9A(ii). The middle section of the confocal stack is presented in Fig 9A(iii), and shows an open lumen lined with MVEC. Fig 9A(iv) shows a histological section of a similar vessel, displaying a hollow lumen lined with stained cells. Serial sections of inosculating vessels from different two adjacent microtissues are shown in Fig 9B. The sequence clearly shows the connection of neovessels, which were observed to traverse relatively long distances (1–2 mm) through the matrix by day 14.

Populations of microtissues were also maintained in suspension cultures (as opposed to being embedded in acellular fibrin matrices). These microtissues aggregated into larger tissue masses over time, as shown in Figure 10. The size of the tissue mass tended to increase with an increase in the initial number of microtissues suspended, and larger masses (>300 μL of initial microtissue volume) were observed to exhibit regions of low cell density in the central regions of the masses, possibly due to cell necrosis caused by a lack of nutrients. Therefore, studies were carried out using tissue masses made with <100 μL of initial microtissue volume to achieve uniform cell distribution. Microtissues with both 1:1 and 1:3 MVEC:FB cell ratios aggregated into macroscopic clusters by day 7. The 1:1 microtissues produced small and diffuse vessels within the clusters (Fig 10A), whereas the vessels produced by the 1:3 microtissues were noticeably larger and formed highly interconnected networks within the clusters (Fig 10B) by day 14. Fluorescence imaging (Fig. 10E) and IHC (Fig. 10F, CD31) of the 1:3 microtissues at day 7 confirmed that the observed vessel formations were produced by MVEC, and also showed a layer of fibroblasts on the external surface of the tissue mass. At day 14, the vessel networks were even less prominent in the 1:1 microtissue masses (Fig. 10C) than at the earlier time point, while in the 1:3 microtissue masses the vessel structures were maintained (Fig. 10D) and suggested a robust network.

Discussion

The ability to establish convective mass transfer in an ischemic tissue or in an engineered tissue construct is an important step toward developing cell-based therapies for a variety of indications. Formation of blood vessels in tissues involves well-orchestrated interactions between cells and the extracellular matrix that are further influenced by biochemical and mechanical cues. Recapitulating the key aspects of this process through the delivery of appropriate cell types and materials is a main goal in vascular tissue engineering. The approach presented here incorporates cells and a permissive matrix to create modular microtissues that mimic the native microenvironment and can be used as a scalable strategy to vascularize tissues. Fabrication of fibrin-based microtissues is rapid and facile, and populations of microtissues can be delivered minimally invasively via injection[63].

The cell types and sources used in vascular tissue engineering are important considerations in developing a therapy, since autologous cells are the most likely to be used clinically. MVEC can be isolated from skin biopsies and therefore offer a readily-available source of autologous cells[28–30]. Furthermore, it has been suggested that the endothelium in microvessels differs from that of larger vessels in ways that makes it particular non-thrombogenic. The basement membrane of microvessels is predominantly comprised of collagen Type IV[64], whereas larger vessels tend to also contain the more thrombogenic collagens (Types I, III, and VI)[25, 65]. Similarly, MVEC may express lower levels of Von Willebrand Factor[22, 57], making them particularly useful in preventing clotting in vessels of small diameter with low flow rates. These characteristics of MVEC make them an attractive cell source for tissue engineering applications, and in particular for revascularization applications.

The importance of supporting perivascular cells in promoting and maintaining new vessel formation has become increasingly clear[66–68]. A variety of cell types have been studied in this role, and the choice of FB in this study was again motivated by the potential of creating a fully autologous therapy. The combination of MVEC and FB in modular fibrin microtissues led to robust endothelial sprouting, both in cell-seeded bulk gels and from cell-laden microtissues embedded in acellular surrounding gels. In the absence of FB, there was essentially no endothelial elongation or sprouting, but both the 1:1 and 1:3 MVEC:FB ratios produced clear sprouts into a surrounding acellular gel over 2–3 days in culture. Both the number and the length of sprouts were positively correlated with an increased proportion of FB in the cultures. The role of FB as a source of soluble paracrine factors involved in vasculogenesis is well established, in particular as related to vascular endothelial growth factor (VEGF)[69], platelet-derived growth factor (PDGF)[70], and transforming growth factor-β (TGF-β,)[71]. In addition, it has been suggested that FB play an important role in modifying and organizing the extracellular matrix[72], and that FB secrete characteristic ECM proteins that promote endothelial tube formation[66, 73–74].

Increasing the volume of medium used to incubate MVEC:FB cultures also tended to increase the number and length of sprouts formed. This effect was more pronounced in the 1:3 MVEC:FB ratio, and may be due to the increased nutrient demand by FB in these cultures, such that access to more nutrients allowed greater cellular activity. It has also been suggested that the proximity of supporting perivascular cells to endothelial cells plays a role in the degree of vasculogenesis[60]. These heterotypic interactions were presumably enhanced in the cultures with a greater proportion of FB. In addition, the observed effects could be ECM-mediated, for example through interactions of pericytes with the ECM, which has been shown to regulate vessel formation[67].

The viability of cells after embedding in microtissues was high (>90%) and comparable to that of cells embedded in similar bulk hydrogels, suggesting that the microtissue fabrication process was not harmful to the cellular component. Subsequent to encapsulation the embedded cells continued to proliferate, as evidenced by a steady increase in DNA content of the microtissues. Quantification of total DNA did not differentiate between cell types, however flow cytometric analysis revealed that FB proliferation accounted for the bulk of the increase in the cell number. In addition, confocal imaging showed that FB were organized around the periphery of endothelial tubes, suggesting a pericyte-like function. It has been shown that sprouting endothelial cells secrete growth factors that result in proliferation and migration of pericytes during maturation[68, 75]. Because the initial total cell number was held constant, the 1:1 microtissues contained more MVEC than the 1:3 microtissues even after two weeks of culture, as inferred through DNA quantification and flow cytometric analysis of cell ratios. It is likely that in this case the increased paracrine signaling between MVEC and FB in the 1:1 microtissues promoted greater FB proliferation, resulting in higher DNA content in these samples at both day 7 and day 14, compared to microtissues with a 1:3 MVEC:FB ratio. It has also been shown that tip cells in particular play a role in pericyte recruitment via PDGF signaling, while lumen formation may be favored when pericytes are more abundant[76–77].

Examination of endothelial sprouting from microtissues revealed that a higher proportion of MVEC (1:1 microtissues) resulted in a greater normalized vessel area at day 7, compared to the 1:3 microtissues. However, by day 14 the vessel area was similar between the conditions, suggesting that the presence of a greater number of FB accelerated the sprouting process. In general, the 1:1 microtissues tended to exhibit a larger number of smaller diameter sprouts initially, relative to the 1:3 microtissues. With a greater proportion of FB (1:3 microtissues), the vessels tended to be larger and mature more rapidly. Examination of vessel diameter showed that the 1:3 microtissues had a wider spread of vessel size, with larger vessels dominating, and that by day 14 the average vessel size was significantly greater than in the 1:1 microtissues. These results suggest that a higher proportion of FB promoted lumen formation and maturation in the form of larger vessels. Therefore variation of the endothelial cell to pericyte ratio may be a tool that can be used to modulate vessel size in engineered tissues, to promote efficient convective flow and mass transfer in hierarchical vascular structures.

Inosculation of vessels from adjoining microtissues is an important process for creating larger vascular networks, and was observed within one week after embedding of microtissues in a surrounding acellular matrix at both MVEC:FB ratios. Further maturation of vessel networks over time was also observed, with clear lumens and branching structures formed by day 14. Serial optical and histological sections confirmed that the inosculation of vessels to form continuous lumens, a process important in forming a functional capillary plexus. When microtissues were cultured in suspension and allowed to aggregate into larger clusters, similar vascular networks were formed within the tissue mass. The effect of a higher proportion of FB was again evident, with the 1:3 microtissues having more robust and stable vessel networks. The creation of vascularized microtissue masses offers the possibility of including parenchymal cells (e.g. hepatocytes, pancreatic cells, myocytes, etc.) in such clusters to generate vascularized organoids. The potential of cell spheroids in engineering tissues has been demonstrated in a variety of applications[78], and vascularization of such structures could improve their utility.

In summary, we have developed and characterized microtissue modules seeded with microvascular endothelial cells and fibroblasts, and have demonstrated their capability to generate capillary sprouts and subsequent interconnected vessel networks *in vitro*. The presence of fibroblasts as supporting perivascular cells was required to achieve endothelial sprouting. A higher proportion of fibroblasts embedded in microtissues favored generation of larger vessels, and the MVEC:FB ratio could potentially be used to tailor vessel characteristics. Use of MVEC and FB in a fibrin matrix offers the possibility of creating a fully autologous cell therapy, and the small size of these modules allows injection of populations of microtissues in a minimally invasive manner. Protein-based microtissues can be readily fabricated and cultured, and such microtissues could find utility as a prevascularization tool for engineered tissues or as a therapy for ischemic disease.

Acknowledgments

Research reported in this publication was supported in part by the National Heart, Lung, and Blood Institute under award numbers R01HL118259 (to AJP and JPS) and the Training Program in Translational Cardiovascular Research and Entrepreneurship (T32HL125242, to AYR), and by the National Institute of Arthritis and

Musculoskeletal and Skin Diseases under award number R01AR062636 (to JPS). The content is solely the responsibility of the authors and does not necessarily represent the official views of the National Institutes of Health.

References

1. Jain RK, Au P, Tam J, Duda DG, Fukumura D. Engineering vascularized tissue. Nature biotechnology. 2005; 23(7):821–3. DOI: 10.1038/nbt0705-821
2. Morgan JP, Delnero PF, Zheng Y, Verbridge SS, Chen J, Craven M, Choi NW, Diaz-Santana A, Kermani P, Hempstead B, Lopez JA, Corso TN, Fischbach C, Stroock AD. Formation of microvascular networks in vitro. Nature protocols. 2013; 8(9):1820–36. DOI: 10.1038/nprot.2013.110 [PubMed: 23989676]
3. Baiguera S, Ribatti D. Endothelialization approaches for viable engineered tissues. Angiogenesis. 2013; 16(1):1–14. DOI: 10.1007/s10456-012-9307-8 [PubMed: 23010872]
4. Laschke MW, Menger MD. Vascularization in tissue engineering: angiogenesis versus inosculation. Eur Surg Res. 2012; 48(2):85–92. DOI: 10.1159/000336876 [PubMed: 22456224]
5. Nichol JW, Khademhosseini A. Modular Tissue Engineering: Engineering Biological Tissues from the Bottom Up. Soft matter. 2009; 5(7):1312–1319. DOI: 10.1039/b814285h [PubMed: 20179781]
6. Tiruvannamalai-Annamalai R, Mertz D, Daley E, Stegemann JP. Collagen Type II Enhances Chondrogenic Differentiation in Agarose-based Modular Microtissues. Cytotherapy. 2016 (In Press).
7. Rao RR, Vigen ML, Peterson AW, Caldwell DJ, Putnam AJ, Stegemann JP. Dual-phase osteogenic and vasculogenic engineered tissue for bone formation. Tissue engineering. Part A. 2015; 21(3–4):530–40. DOI: 10.1089/ten.TEA.2013.0740 [PubMed: 25228401]
8. Wang MO, Vorwald CE, Dreher ML, Mott EJ, Cheng MH, Cinar A, Mehdizadeh H, Somo S, Dean D, Brey EM, Fisher JP. Evaluating 3D-printed biomaterials as scaffolds for vascularized bone tissue engineering. Adv Mater. 2015; 27(1):138–44. DOI: 10.1002/adma.201403943 [PubMed: 25387454]
9. Daley ELH, Coleman RM, Stegemann JP. Biomimetic microbeads containing a chondroitin sulfate/chitosan polyelectrolyte complex for cell-based cartilage therapy. Journal of Materials Chemistry B. 2015; 3(40):7920–7929. DOI: 10.1039/C5TB00934K [PubMed: 26693016]
10. Riesberg JJ, Shen W. A biological approach to assembling tissue modules through endothelial capillary network formation. Journal of tissue engineering and regenerative medicine. 2015; 9(9):1084–1087. DOI: 10.1002/term.2008 [PubMed: 25694020]
11. Tiruvannamalai-Annamalai R, Armant DR, Matthew HW. A glycosaminoglycan based, modular tissue scaffold system for rapid assembly of perfusable, high cell density, engineered tissues. PloS one. 2014; 9(1):e84287.doi: 10.1371/journal.pone.0084287 [PubMed: 24465401]
12. McGuigan AP, Sefton MV. Vascularized organoid engineered by modular assembly enables blood perfusion. Proceedings of the National Academy of Sciences of the United States of America. 2006; 103(31):11461–6. DOI: 10.1073/pnas.0602740103 [PubMed: 16864785]
13. Rioja AY, Tiruvannamalai Annamalai R, Paris S, Putnam AJ, Stegemann JP. Endothelial sprouting and network formation in collagen- and fibrin-based modular microbeads. Acta biomaterialia. 2016; 29:33–41. DOI: http://dx.doi.org/10.1016/j.actbio.2015.10.022. [PubMed: 26481042]
14. Peterson AW, Caldwell DJ, Rioja AY, Rao RR, Putnam AJ, Stegemann JP. Vasculogenesis and Angiogenesis in Modular Collagen-Fibrin Microtissues. Biomaterials science. 2014; 2(10):1497–1508. DOI: 10.1039/C4BM00141A [PubMed: 25177487]
15. Ye X, Lu L, Kolewe ME, Park H, Larson BL, Kim ES, Freed LE. A biodegradable microvessel scaffold as a framework to enable vascular support of engineered tissues. Biomaterials. 2013; 34(38):10007–15. DOI: 10.1016/j.biomaterials.2013.09.039 [PubMed: 24079890]
16. Risau W. Mechanisms of angiogenesis. Nature. 1997; 386(6626):671–4. DOI: 10.1038/386671a0 [PubMed: 9109485]
17. Carmeliet P. Mechanisms of angiogenesis and arteriogenesis. Nat Med. 2000; 6(4):389–95. DOI: 10.1038/74651 [PubMed: 10742145]
18. Risau W, Flamme I. Vasculogenesis. Annual review of cell and developmental biology. 1995; 11(1):73–91. DOI: 10.1146/annurev.cb.11.110195.000445

19. Patan S. Vasculogenesis and Angiogenesis as Mechanisms of Vascular Network Formation, Growth and Remodeling. Journal of Neuro-Oncology. 2000; 50(1–2):1–15. DOI: 10.1023/A:1006493130855 [PubMed: 11245270]
20. Karamysheva AF. Mechanisms of angiogenesis. Biochemistry Moscow. 2008; 73(7):751–762. DOI: 10.1134/S0006297908070031 [PubMed: 18707583]
21. Kutcher ME, Herman IM. The pericyte: Cellular regulator of microvascular blood flow. Microvascular research. 2009; 77(3):235–246. DOI: http://dx.doi.org/10.1016/j.mvr.2009.01.007. [PubMed: 19323975]
22. Bergers G, Song S. The role of pericytes in blood-vessel formation and maintenance. Neuro-Oncology. 2005; 7(4):452–464. DOI: 10.1215/S1152851705000232 [PubMed: 16212810]
23. Kniazeva E, Kachgal S, Putnam AJ. Effects of Extracellular Matrix Density and Mesenchymal Stem Cells on Neovascularization In Vivo. Tissue Engineering Part A. 2010; 17(7–8):905–914. DOI: 10.1089/ten.tea.2010.0275 [PubMed: 20979533]
24. Hegen A, Blois A, Tiron CE, Hellesøy M, Micklem DR, Nör JE, Akslen LA, Lorens JB. Efficient in vivo Vascularization of Tissue Engineering Scaffolds. Journal of tissue engineering and regenerative medicine. 2011; 5(4):e52–e62. DOI: 10.1002/term.336 [PubMed: 20865694]
25. Yamamoto K, de Waard V, Fearns C, Loskutoff DJ. Tissue distribution and regulation of murine von Willebrand factor gene expression in vivo. Blood. 1998; 92(8):2791–801. [PubMed: 9763564]
26. Bonnefoy A, Harsfalvi J, Pfliegler G, Fauvel-Lafeve F, Legrand C. The subendothelium of the HMEC-1 cell line supports thrombus formation in the absence of von Willebrand factor and collagen types I, III and VI. Thrombosis and haemostasis. 2001; 85(3):552–9. [PubMed: 11307830]
27. Tannenbaum SH, Rick ME, Shafer B, Gralnick HR. Subendothelial matrix of cultured endothelial cells contains fully processed high molecular weight von Willebrand factor. J Lab Clin Med. 1989; 113(3):372–8. [PubMed: 2784474]
28. Normand J, Karasek MA. A method for the isolation and serial propagation of keratinocytes, endothelial cells, and fibroblasts from a single punch biopsy of human skin. In Vitro Cell Dev Biol - Animal. 1995; 31(6):447–455. DOI: 10.1007/BF02634257
29. Rafii S, Shapiro F, Rimarachin J, Nachman R, Ferris B, Weksler B, Moore M, Asch A. Isolation and characterization of human bone marrow microvascular endothelial cells: hematopoietic progenitor cell adhesion. Blood. 1994; 84(1):10–19. [PubMed: 7517203]
30. Gargett CE, Bucak K, Rogers PA. Isolation, characterization and long-term culture of human myometrial microvascular endothelial cells. Hum Reprod. 2000; 15(2):293–301. [PubMed: 10655298]
31. Nair, L., Laurencin, C. Polymers as Biomaterials for Tissue Engineering and Controlled Drug Delivery. In: Lee, K., Kaplan, D., editors. Tissue Engineering I. Vol. 102. Springer; Berlin Heidelberg: 2006. p. 47-90.
32. Feng X, Clark RAF, Galanakis D, Tonnesen MG. Fibrin and Collagen Differentially Regulate Human Dermal Microvascular Endothelial Cell Integrins: Stabilization of αv/β3 mRNA by Fibrin1. Journal of Investigative Dermatology. 1999; 113(6):913–919. DOI: http://dx.doi.org/10.1046/j.1523-1747.1999.00786.x. [PubMed: 10594730]
33. Ahmed TA, Dare EV, Hincke M. Fibrin: a versatile scaffold for tissue engineering applications. Tissue engineering. Part B, Reviews. 2008; 14(2):199–215. DOI: 10.1089/ten.teb.2007.0435 [PubMed: 18544016]
34. Ceccarelli J, Putnam AJ. Sculpting the blank slate: How fibrin's support of vascularization can inspire biomaterial design. Acta biomaterialia. 2014; 10(4):1515–1523. DOI: http://dx.doi.org/10.1016/j.actbio.2013.07.043. [PubMed: 23933102]
35. Mosesson MW, Siebenlist KR, Meh DA. The structure and biological features of fibrinogen and fibrin. Annals of the New York Academy of Sciences. 2001; 936:11–30. [PubMed: 11460466]
36. Aper T, Schmidt A, Duchrow M, Bruch HP. Autologous Blood Vessels Engineered from Peripheral Blood Sample. European Journal of Vascular and Endovascular Surgery. 2007; 33(1):33–39. DOI: http://dx.doi.org/10.1016/j.ejvs.2006.08.008. [PubMed: 17070080]
37. Kneser U, Stangenberg L, Ohnolz J, Buettner O, Stern-Straeter J, Möbest D, Horch RE, Stark GB, Schaefer DJ. Evaluation of processed bovine cancellous bone matrix seeded with syngenic

osteoblasts in a critical size calvarial defect rat model. Journal of Cellular and Molecular Medicine. 2006; 10(3):695–707. DOI: 10.1111/j.1582-4934.2006.tb00429.x [PubMed: 16989729]

38. Steffens L, Wenger A, Stark GB, Finkenzeller G. In vivo engineering of a human vasculature for bone tissue engineering applications. Journal of Cellular and Molecular Medicine. 2009; 13(9b): 3380–3386. DOI: 10.1111/j.1582-4934.2008.00418.x [PubMed: 18624770]
39. Tan H, Yang B, Duan X, Wang F, Zhang Y, Jin X, Dai G, Yang L. The promotion of the vascularization of decalcified bone matrix in vivo by rabbit bone marrow mononuclear cell-derived endothelial cells. Biomaterials. 2009; 30(21):3560–3566. DOI: http://dx.doi.org/10.1016/j.biomaterials.2009.03.029. [PubMed: 19359037]
40. Murphy KC, Fang SY, Leach JK. Human mesenchymal stem cell spheroids in fibrin hydrogels exhibit improved cell survival and potential for bone healing. Cell and tissue research. 2014; 357(1):91–99. DOI: 10.1007/s00441-014-1830-z [PubMed: 24781147]
41. Neumeister MW, Wu T, Chambers C. Vascularized tissue-engineered ears. Plastic and reconstructive surgery. 2006; 117(1):116–22. [PubMed: 16404257]
42. Ishak, MFb, See, GB., Hui, CK., Abdullah, Ab, Saim, Lb, Saim, Ab, Idrus, RbH. The formation of human auricular cartilage from microtic tissue: An in vivo study. International journal of pediatric otorhinolaryngology. 2015; 79(10):1634–1639. DOI: http://dx.doi.org/10.1016/j.ijporl.2015.06.034. [PubMed: 26250439]
43. Abdul Rahman R, Mohamad Sukri N, Md Nazir N, Ahmad Radzi MAz, Zulkifly AH, Che Ahmad A, Hashi AA, Abdul Rahman S, Sha'ban M. The potential of 3-dimensional construct engineered from poly(lactic-co-glycolic acid)/fibrin hybrid scaffold seeded with bone marrow mesenchymal stem cells for in vitro cartilage tissue engineering. Tissue and Cell. 2015; 47(4):420–430. DOI: http://dx.doi.org/10.1016/j.tice.2015.06.001. [PubMed: 26100682]
44. Verseijden F, Posthumus-van Sluijs SJ, van Neck JW, Hofer SO, Hovius SE, van Osch GJ. Vascularization of prevascularized and non-prevascularized fibrin-based human adipose tissue constructs after implantation in nude mice. Journal of tissue engineering and regenerative medicine. 2012; 6(3):169–78. DOI: 10.1002/term.410 [PubMed: 21360688]
45. Wittmann K, Dietl S, Ludwig N, Berberich O, Hoefner C, Storck K, Blunk T, Bauer-Kreisel P. Engineering vascularized adipose tissue using the stromal-vascular fraction and fibrin hydrogels. Tissue engineering. Part A. 2015; 21(7–8):1343–53. DOI: 10.1089/ten.TEA.2014.0299 [PubMed: 25602488]
46. Wittmann K, Storck K, Muhr C, Mayer H, Regn S, Staudenmaier R, Wiese H, Maier G, Bauer-Kreisel P, Blunk T. Development of volume-stable adipose tissue constructs using polycaprolactone-based polyurethane scaffolds and fibrin hydrogels. Journal of tissue engineering and regenerative medicine. 2013; doi: 10.1002/term.1830
47. Fiegel HC, Pryymachuk G, Rath S, Bleiziffer O, Beier JP, Bruns H, Kluth D, Metzger R, Horch RE, Till H, Kneser U. Foetal hepatocyte transplantation in a vascularized AV-Loop transplantation model in the rat. Journal of Cellular and Molecular Medicine. 2010; 14(1–2):267–274. DOI: 10.1111/j.1582-4934.2008.00369.x [PubMed: 18505475]
48. Riopel M, Trinder M, Wang R. Fibrin, a Scaffold Material for Islet Transplantation and Pancreatic Endocrine Tissue Engineering. Tissue Engineering Part B: Reviews. 2014; 21(1):34–44. DOI: 10.1089/ten.teb.2014.0188 [PubMed: 24947304]
49. Lugo LM, Lei P, Andreadis ST. Vascularization of the Dermal Support Enhances Wound Re-Epithelialization by In Situ Delivery of Epidermal Keratinocytes. Tissue Engineering Part A. 2010; 17(5–6):665–675. DOI: 10.1089/ten.tea.2010.0125 [PubMed: 20929281]
50. Montaño I, Schiestl C, Schneider J, Pontiggia L, Luginbühl J, Biedermann T, Böttcher-Haberzeth S, Braziulis E, Meuli M, Reichmann E. Formation of Human Capillaries In Vitro: The Engineering of Prevascularized Matrices. Tissue Engineering Part A. 2009; 16(1):269–282. DOI: 10.1089/ten.tea.2008.0550
51. Liao H, Zhou G-Q. Development and Progress of Engineering of Skeletal Muscle Tissue. Tissue Engineering Part B: Reviews. 2009; 15(3):319–331. DOI: 10.1089/ten.teb.2009.0092 [PubMed: 19591626]
52. Schmidt D, Hoerstrup SP. Tissue engineered heart valves based on human cells. Swiss Med Wkly. 2006; 136(39–40):618–23. 2006/39/smw-11400. [PubMed: 17086507]

53. Flanagan TC, Sachweh JS, Frese J, Schnoring H, Gronloh N, Koch S, Tolba RH, Schmitz-Rode T, Jockenhoevel S. In vivo remodeling and structural characterization of fibrin-based tissue-engineered heart valves in the adult sheep model. Tissue engineering. Part A. 2009; 15(10):2965–76. DOI: 10.1089/ten.TEA.2009.0018 [PubMed: 19320544]
54. Chung E, Rytlewski JA, Merchant AG, Dhada KS, Lewis EW, Suggs LJ. Fibrin-based 3D matrices induce angiogenic behavior of adipose-derived stem cells. Acta biomaterialia. 2015; 17:78–88. DOI: http://dx.doi.org/10.1016/j.actbio.2015.01.012. [PubMed: 25600400]
55. Riemenschneider SB, Mattia DJ, Wendel JS, Schaefer JA, Ye L, Guzman PA, Tranquillo RT. Inosculation and perfusion of pre-vascularized tissue patches containing aligned human microvessels after myocardial infarction. Biomaterials. 2016; 97:51–61. DOI: http://dx.doi.org/10.1016/j.biomaterials.2016.04.031. [PubMed: 27162074]
56. Ghajar CM, Blevins KS, Hughes CC, George SC, Putnam AJ. Mesenchymal stem cells enhance angiogenesis in mechanically viable prevascularized tissues via early matrix metalloproteinase upregulation. Tissue engineering. 2006; 12(10):2875–88. DOI: 10.1089/ten.2006.12.2875 [PubMed: 17518656]
57. Rowe SL, Lee S, Stegemann JP. Influence of thrombin concentration on the mechanical and morphological properties of cell-seeded fibrin hydrogels. Acta biomaterialia. 2007; 3(1):59–67. DOI: http://dx.doi.org/10.1016/j.actbio.2006.08.006. [PubMed: 17085089]
58. Lorentz KM, Kontos S, Frey P, Hubbell JA. Engineered aprotinin for improved stability of fibrin biomaterials. Biomaterials. 2011; 32(2):430–438. DOI: http://dx.doi.org/10.1016/j.biomaterials.2010.08.109. [PubMed: 20864171]
59. Liu H, Collins SF, Suggs LJ. Three-dimensional culture for expansion and differentiation of mouse embryonic stem cells. Biomaterials. 2006; 27(36):6004–6014. DOI: http://dx.doi.org/10.1016/j.biomaterials.2006.06.016. [PubMed: 16860386]
60. Griffith CK, Miller C, Sainson RC, Calvert JW, Jeon NL, Hughes CC, George SC. Diffusion limits of an in vitro thick prevascularized tissue. Tissue engineering. 2005; 11(1–2):257–66. DOI: 10.1089/ten.2005.11.257 [PubMed: 15738680]
61. Ghajar CM, Chen X, Harris JW, Suresh V, Hughes CC, Jeon NL, Putnam AJ, George SC. The effect of matrix density on the regulation of 3-D capillary morphogenesis. Biophysical journal. 2008; 94(5):1930–41. DOI: 10.1529/biophysj.107.120774 [PubMed: 17993494]
62. Chen XF, Aledia AS, Ghajar CM, Griffith CK, Putnam AJ, Hughes CCW, George SC. Prevascularization of a Fibrin-Based Tissue Construct Accelerates the Formation of Functional Anastomosis with Host Vasculature. Tissue Engineering Part A. 2009; 15(6):1363–1371. DOI: 10.1089/ten.tea.2008.0314 [PubMed: 18976155]
63. Wang L, Rao RR, Stegemann JP. Delivery of Mesenchymal Stem Cells in Chitosan/Collagen Microbeads for Orthopedic Tissue Repair. Cells, tissues, organs. 2013; 197(5):333–343. [PubMed: 23571151]
64. Yurchenco PD, Schittny JC. Molecular architecture of basement membranes. FASEB journal : official publication of the Federation of American Societies for Experimental Biology. 1990; 4(6): 1577–90. [PubMed: 2180767]
65. Gerritsen ME. Functional heterogeneity of vascular endothelial cells. Biochem Pharmacol. 1987; 36(17):2701–11. [PubMed: 2820420]
66. Newman AC, Nakatsu MN, Chou W, Gershon PD, Hughes CC. The requirement for fibroblasts in angiogenesis: fibroblast-derived matrix proteins are essential for endothelial cell lumen formation. Molecular biology of the cell. 2011; 22(20):3791–800. DOI: 10.1091/mbc.E11-05-0393 [PubMed: 21865599]
67. Carrion B, Kong YP, Kaigler D, Putnam AJ. Bone marrow-derived mesenchymal stem cells enhance angiogenesis via their α6β1 integrin receptor. Experimental cell research. 2013; 319(19): 2964–2976. DOI: http://dx.doi.org/10.1016/j.yexcr.2013.09.007. [PubMed: 24056178]
68. Armulik A, Abramsson A, Betsholtz C. Endothelial/pericyte interactions. Circ Res. 2005; 97(6): 512–23. DOI: 10.1161/01.RES.0000182903.16652.d7 [PubMed: 16166562]
69. Kellouche S, Mourah S, Bonnefoy A, Schoevaert D, Podgorniak MP, Calvo F, Hoylaerts MF, Legrand C, Dosquet C. Platelets, thrombospondin-1 and human dermal fibroblasts cooperate for

stimulation of endothelial cell tubulogenesis through VEGF and PAI-1 regulation. Experimental cell research. 2007; 313(3):486–99. DOI: 10.1016/j.yexcr.2006.10.023 [PubMed: 17126831]

70. Antoniades HN, Galanopoulos T, Neville-Golden J, Kiritsy CP, Lynch SE. Injury induces in vivo expression of platelet-derived growth factor (PDGF) and PDGF receptor mRNAs in skin epithelial cells and PDGF mRNA in connective tissue fibroblasts. Proceedings of the National Academy of Sciences of the United States of America. 1991; 88(2):565–9. [PubMed: 1846446]
71. Paunescu V, Bojin FM, Tatu CA, Gavriliuc OI, Rosca A, Gruia AT, Tanasie G, Bunu C, Crisnic D, Gherghiceanu M, Tatu FR, Tatu CS, Vermesan S. Tumour-associated fibroblasts and mesenchymal stem cells: more similarities than differences. J Cell Mol Med. 2011; 15(3):635–46. DOI: 10.1111/j.1582-4934.2010.01044.x [PubMed: 20184663]
72. Chang HY, Chi JT, Dudoit S, Bondre C, van de Rijn M, Botstein D, Brown PO. Diversity, topographic differentiation, and positional memory in human fibroblasts. Proceedings of the National Academy of Sciences of the United States of America. 2002; 99(20):12877–82. DOI: 10.1073/pnas.162488599 [PubMed: 12297622]
73. Berthod F, Germain L, Tremblay N, Auger FA. Extracellular matrix deposition by fibroblasts is necessary to promote capillary-like tube formation in vitro. Journal of cellular physiology. 2006; 207(2):491–498. DOI: 10.1002/jcp.20584 [PubMed: 16453301]
74. Nakatsu MN, Sainson RC, Aoto JN, Taylor KL, Aitkenhead M, Perez-del-Pulgar S, Carpenter PM, Hughes CC. Angiogenic sprouting and capillary lumen formation modeled by human umbilical vein endothelial cells (HUVEC) in fibrin gels: the role of fibroblasts and Angiopoietin-1. Microvascular research. 2003; 66(2):102–12. [PubMed: 12935768]
75. Hoch RV, Soriano P. Roles of PDGF in animal development. Development. 2003; 130(20):4769–4784. DOI: 10.1242/dev.00721 [PubMed: 12952899]
76. Hellstrom M, Kal nM, Lindahl P, Abramsson A, Betsholtz C. Role of PDGF-B and PDGFR-beta in recruitment of vascular smooth muscle cells and pericytes during embryonic blood vessel formation in the mouse. Development. 1999; 126(14):3047–3055. [PubMed: 10375497]
77. Adams RH, Alitalo K. Molecular regulation of angiogenesis and lymphangiogenesis. Nat Rev Mol Cell Bio. 2007; 8(6):464–478. [PubMed: 17522591]
78. Gentile C. Filling the Gaps between the In Vivo and In Vitro Microenvironment: Engineering of Spheroids for Stem Cell Technology. Current stem cell research & therapy. 2015

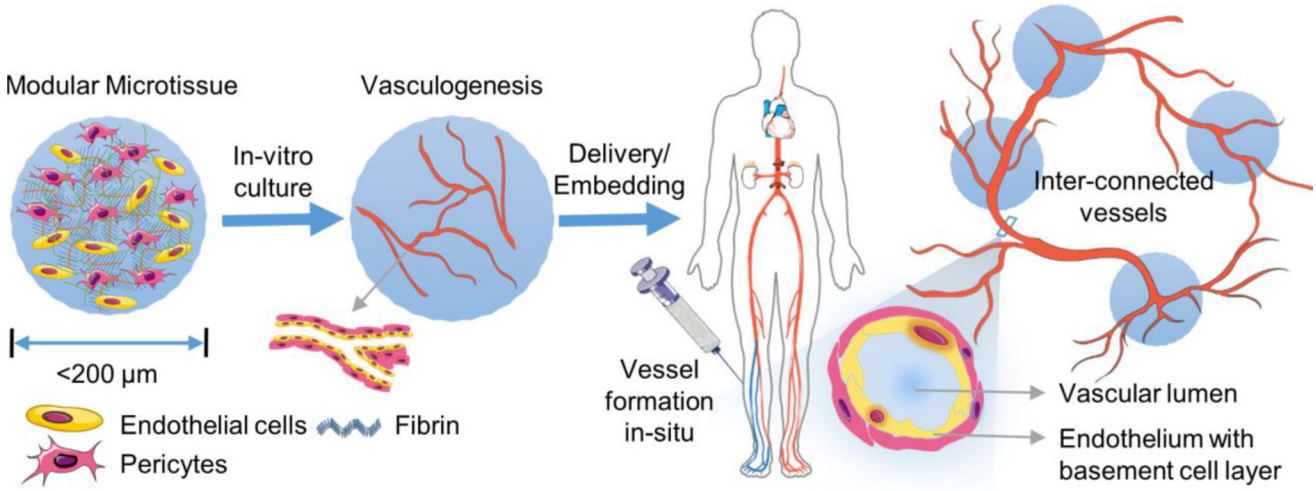

Figure 1.

Schematic of a strategy to treat ischemic tissue with modular microtissues containing embedded endothelial cells and supporting perivascular cells.

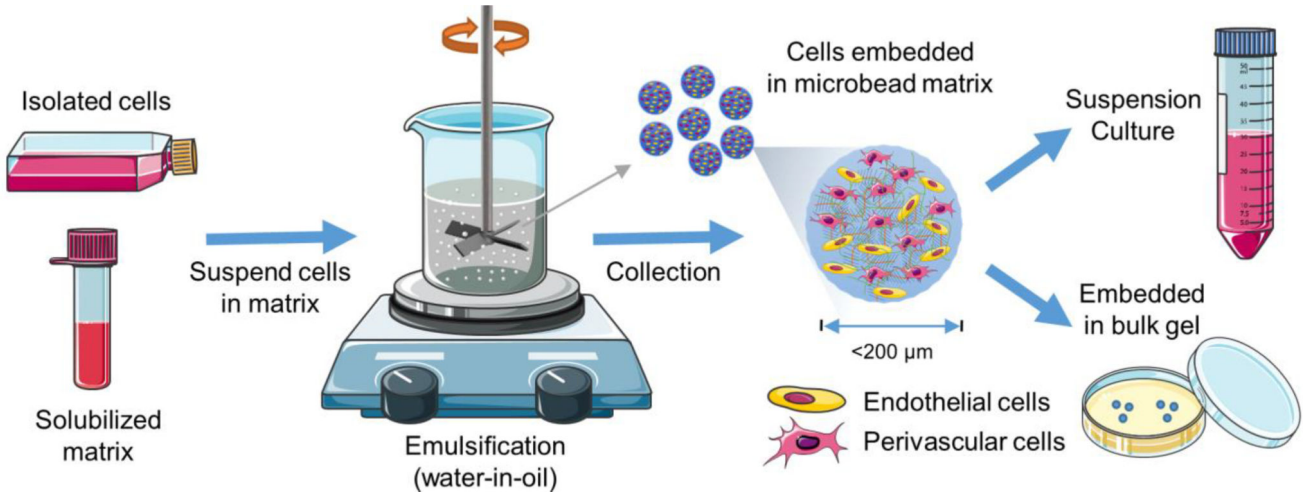

Figure 2.
Schematic of microtissue fabrication process.

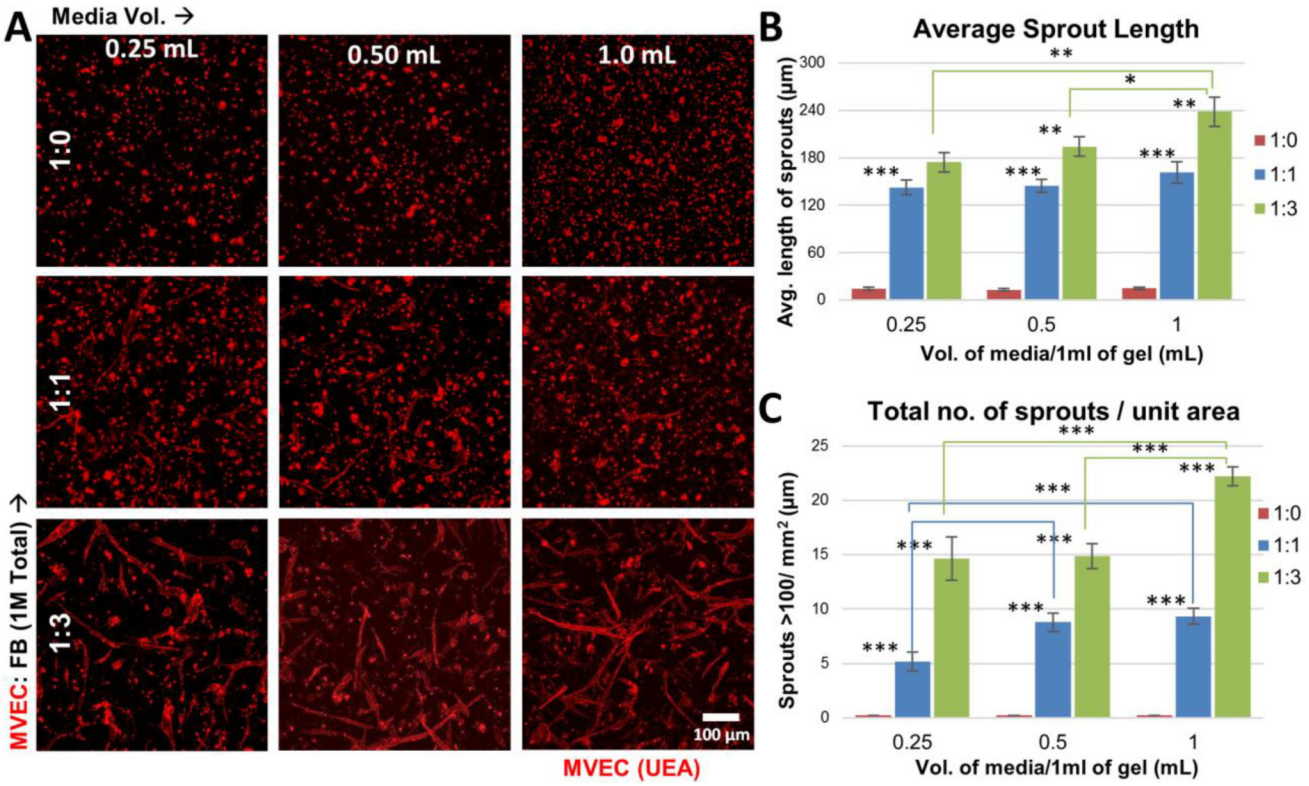

Figure 3.

Endothelial sprouting in bulk fibrin hydrogels. A) Fluorescent images of embedded MVEC stained red with UEA-1 in gels made with different MVEC:FB ratios and cultured in different medium volumes. B) Quantitation of the average sprout length in bulk gels (n=3). C) Quantitation of the number of sprouts >100 µm in length in bulk gels (n=3). Error bars represent standard deviation of the mean. * indicates statistical significance (*p<0.05, **p<0.01 and ***p<0.001).

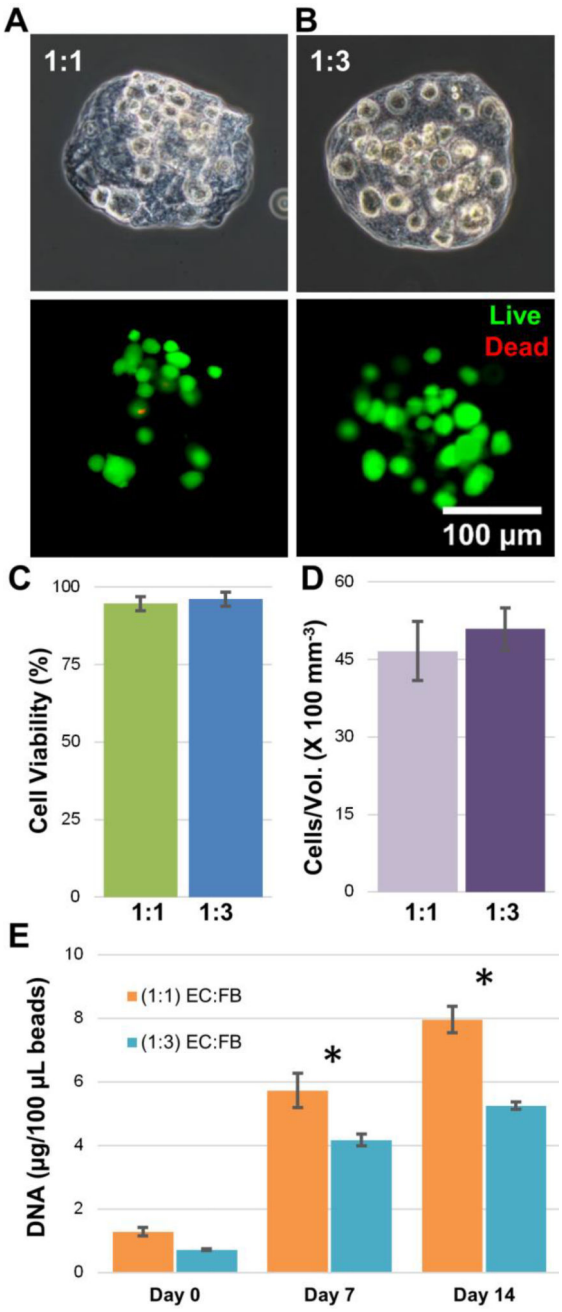

Figure 4.

Characterization of modular microtissues. A) Single MVEC:FB microtissues (1:1 and 1:3) under phase contrast showing microtissue morphology and embedded cells immediately after microbead fabrication. B) Single MVEC:FB microtissues (1:1 and 1:3) under fluorescence showing cell viability (green = live cells, red = dead cells). C) Quantitation of cell viability for a population of microtissues. D) Quantitation of total cells per unit volume for a population of microtissues. E) Total DNA in microtissues as a function of time. Best viewed in color. Error bars represent standard deviation of the mean. * indicates statistical significance (*$p<0.05$).

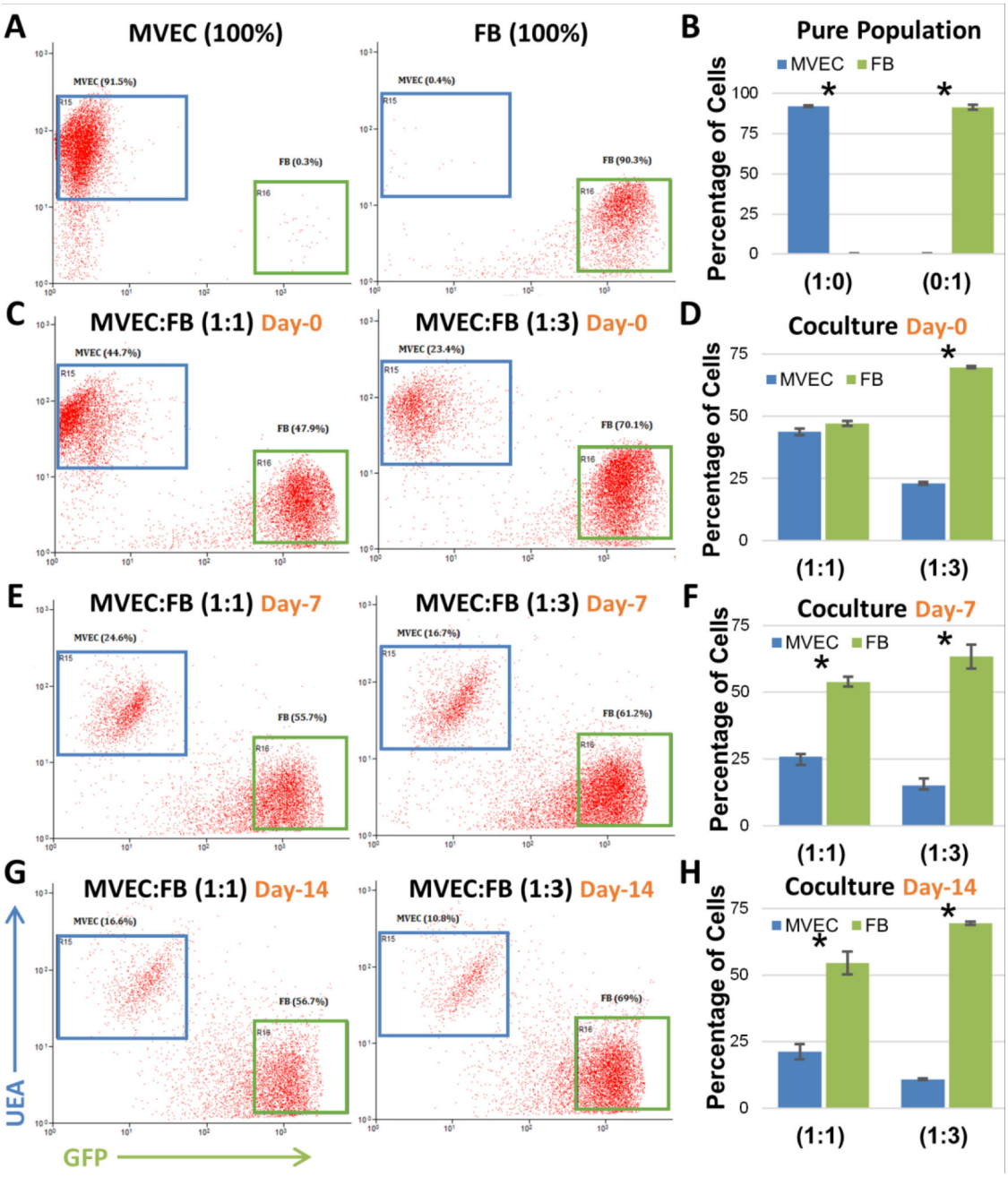

Figure 5.

Flow cytometry analysis of MVEC and FB cell population in fibrin co-cultures over time. A,B) Mono-culture of MVEC and FB. C- H) MVEC and FB cell population in co-cultures over time. Error bars represent standard deviation of the mean. * indicates statistical significance (*p<0.01).

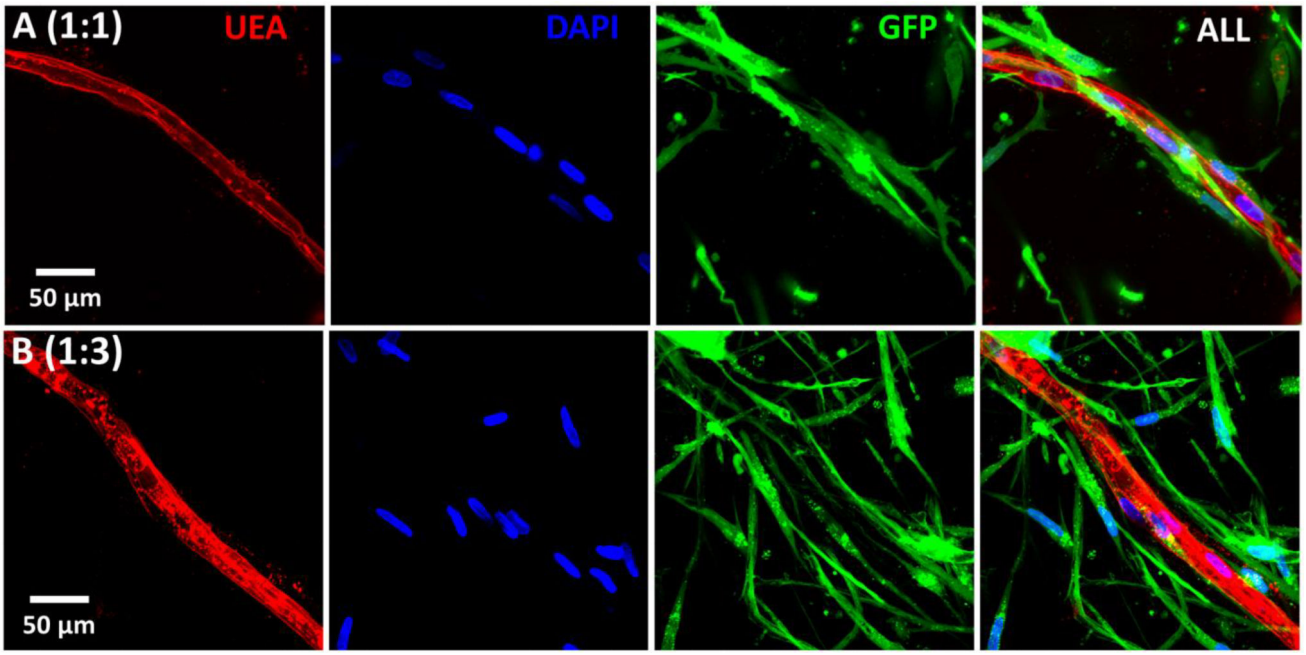

Figure 6.
Maximum intensity projections of confocal stacks showing FB enveloping endothelial vessel surface (Day 14).

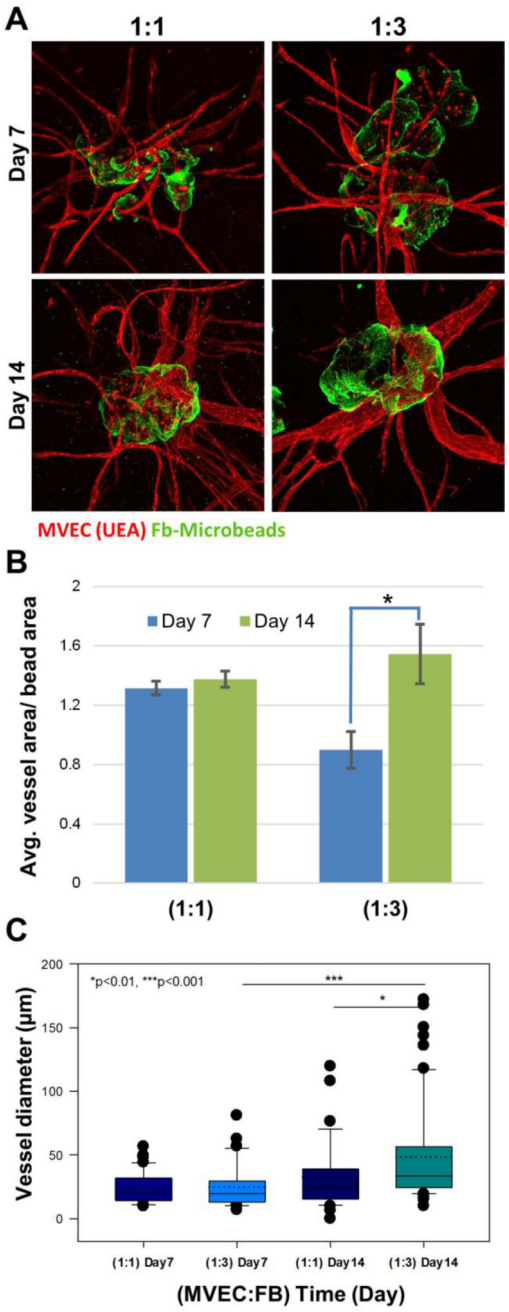

Figure 7.

Sprouting of neovessels from modular microtissues. A) Fluorescence images (green = fibrin, red = MVEC) at day 7 and 14 with different MVEC:FB ratios. B) Quantification of vessel area normalized to microtissue area. C) Box plot of vessel diameter. The solid center line in the box plot represents the median, the dotted center line in the box represents the mean, and the lower and upper boundaries of the box represent the 25th and 75th percentiles, respectively. Whiskers (error bars) above and below the box indicate the 90th and 10th percentiles. Large dots represent outliers.

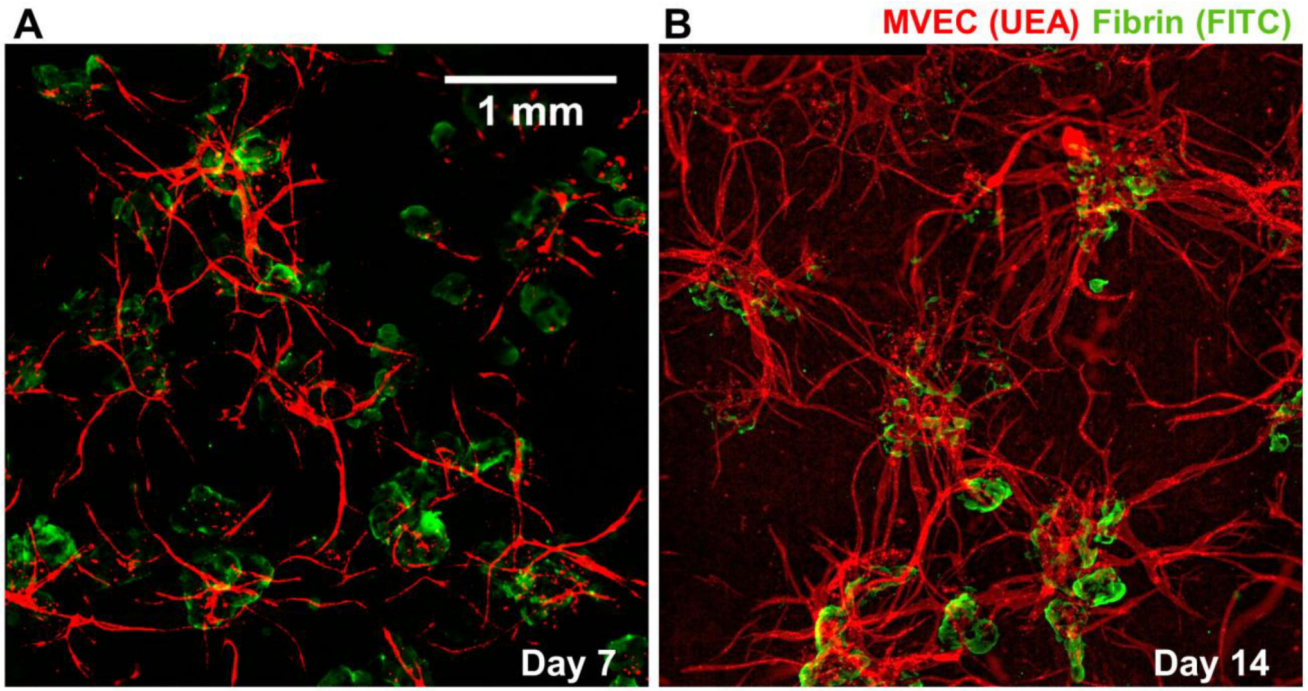

Figure 8.

Fluorescence images showing vessel network (red) formation in between microtissues (green) embedded in a surrounding acellular fibrin hydrogel. Best viewed in color.

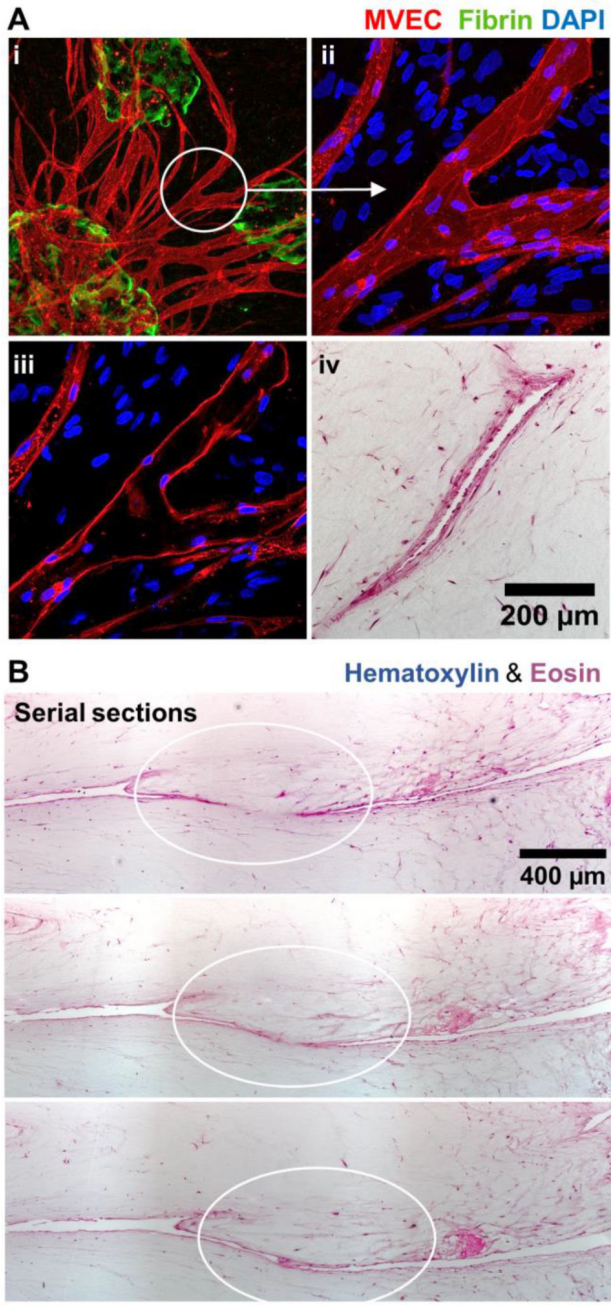

Figure 9.

Inosculation of MVEC neovessels. A) MVEC (red) networks (i) sprouted from microtissues (green) and formed branches (ii) with hollow lumens (iii, iv). B) Serial histological sections showed inosculation of adjacent MVEC vessels.

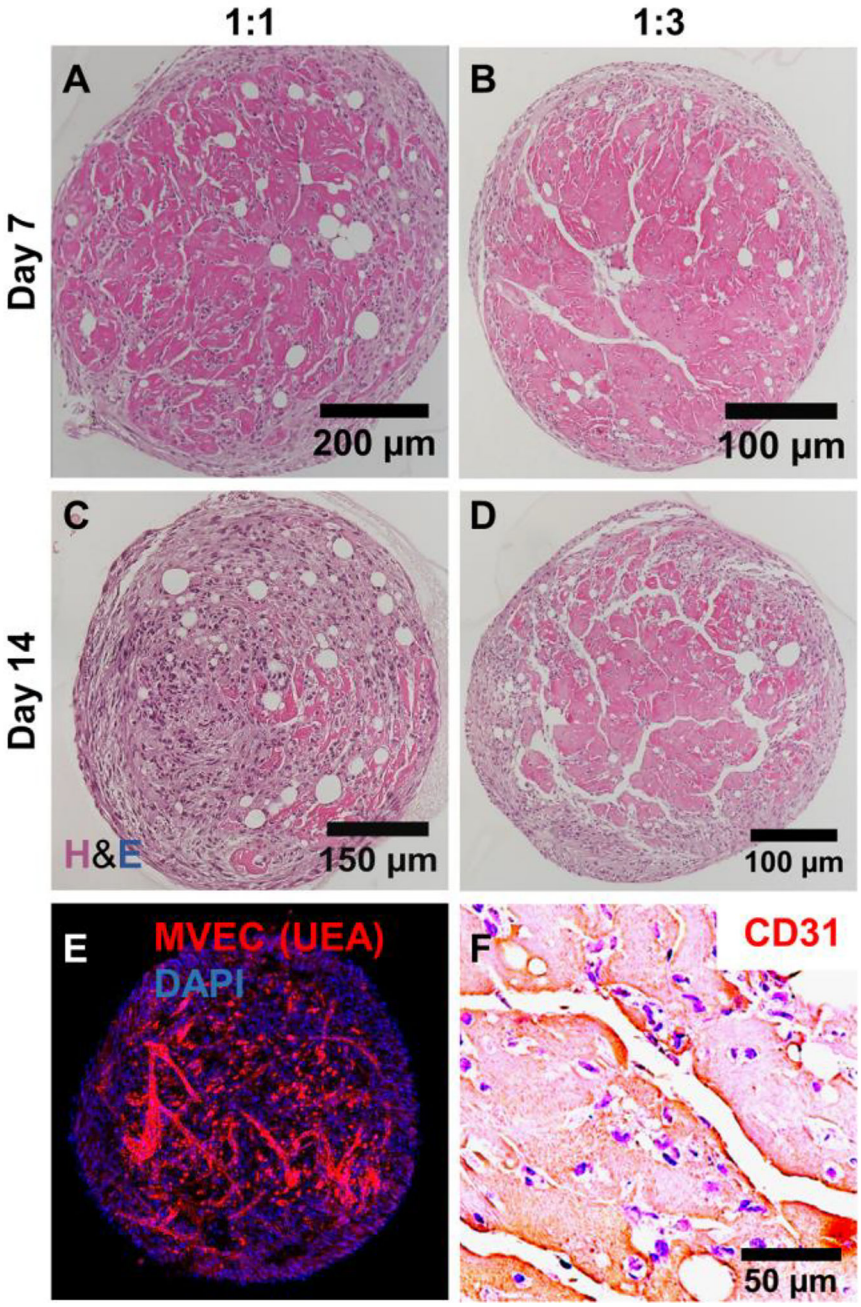

Figure 10.

Microtissues cultured in suspension aggregated to form larger tissue structures. A, B) By day 7, neovessels were evident in tissue masses. C, D) By day 14, networks of vessels had formed in tissue masses made with 1:3 MVEC:FB microtissues, but were less evident in those made at 1:1. E) Fluorescence staining and F) PECAM/CD-31 IHC confirmed that vessels within tissue structures were created by MVEC.

Table I

Influence of cell ratios and culture media volume on total sprouts.

Media volume.	**No of sprouts/unit area (>100 μm)**			**Cell ratio vs. No. of sprouts***
MVEC:FB →	1: 0	1:1	1:3	*r*
0.25	0.2±0	5.2±0.8	14.7±2.0	***−0.762***
0.5	0.2±0	8.8±0.8	14.9±1.1	***−0.910***
1	0.2±0	9.3±0.7	22.2±0.9	***−0.812***
*Media vol vs No of sprouts**	–	***0.829***	***0.953***	

*Pearson correlation coefficients

Table II

Influence of cell ratios and culture media volume on average sprout length.

Media volume	**Average sprout length ± Std Error (μm)**			**Cell ratio vs. Length***
MVEC:FB →	1:0	1:1	1:3	*r*
0.25	14.1±9.5	142.5±9.5	172.3±12.1	***−0.982***
0.5	9.4±1.5	166.6±8.4	194.1±12.3	***−0.967***
1	14.7±1.4	161.2±13.6	238.3±18.2	***−0.941***
*Media vol vs. Length**	***0.286***	***0.974***	***0.999#***	

*Pearson correlation coefficients,

#p<0.01

Table III

Vessel lumen diameter at day 7 and day 14 in embedded microtissue cultures

(MVEC:FB)_Day	Dia. (μm)	Dia. of top 50% (μm)
(1:1)_Day 7	23.7 ± 12.1	31.4 ± 11.0
(1:3)_Day 7	24.9 ± 17.7	37.3 ± 18.4
(1:1)_Day 14	32.7 ± 25.9	50.3 ± 28.7
(1:3)_Day 14	48.4 ± 38.0	73.4 ± 41.1